JOURNAL OF SOLID STATE CHEMISTRY 78, 23–34 (1989)

A Magic Angle Spinning NMR Study of the Phase Diagram $Ca_{3-x}Zn_x(PO_4)_2$

R. J. B. JAKEMAN AND A. K. CHEETHAM*

Chemical Crystallography Laboratory, University of Oxford, 9 Parks Road, Oxford OX1 3PD, United Kingdom

AND N. J. CLAYDEN AND C. M. DOBSON

Inorganic Chemistry Laboratory, University of Oxford, South Parks Road, Oxford OX1 3QR, United Kingdom

Received March 17, 1988; in revised form July 18, 1988

The phase diagram $Ca_{3-x}Zn_x(PO_4)_2$ has been investigated by ^{31}P magic angle spinning NMR (MASNMR). The study demonstrates how MASNMR can be used to make clear distinction between regions of solid solution, line phases, and biphasic mixtures. The ^{31}P MASNMR spectrum of the complex phosphate, β-$Ca_3(PO_4)_2$, has been rationalized in terms of the known structure, and the broadness of the observed resonances has been attributed to the disorder caused by partial occupancy of one metal site. Variations in intensity and linewidth of the ^{31}P MASNMR resonances, as zinc is substituted for calcium in the β-$Ca_3(PO_4)_2$ framework to form a solid solution, have been interpreted by analogy with the isomorphous solid solution $Ca_{3-x}Mg_x(PO_4)_2$. The intermediate phase α-$CaZn_2(PO_4)_2$ has been identified as having no solubility in either end member and is characterized by two distinct isotropic resonances at 10.0 and 2.2 ppm. The spectra of a high-temperature form of each of $Ca_3(PO_4)_2$, $CaZn_2(PO_4)_2$, and $Zn_3(PO_4)_2$ have also been observed.

Introduction

Magic angle spinning NMR (MASNMR) is now established as a technique with wide applicability to problems in solid state chemistry. A number of studies have shown that chemical shift values are sensitive to a variety of structural features. The chemical shift of ^{27}Al in aluminosilicates, for example, is sensitive to coordination number, can be used to distinguish between tetrahedral and octahedral sites (*1*), and has recently been shown to be sensitive to Al–O–Si average bond angles (*2*). In a similar way ^{29}Si chemical shifts can distinguish between crystallographically inequivalent silicon atoms (*3*) as well as being sensitive to slight changes in the local environment, such as the presence of next-nearest aluminiums (*4*). Chemical shift differences have also been expressed in terms of an empirical correlation with the summed bond strength of the oxygens of SiO_4 units in silicates (*5*) studied by ^{29}Si MASNMR or PO_4 units in phosphates (*6*) (^{31}P MASNMR). We have previously demonstrated the sensitivity of ^{31}P MASNMR isotopic chemical shifts to the local environ-

* To whom correspondence should be addressed.

0022-4596/89 $3.00

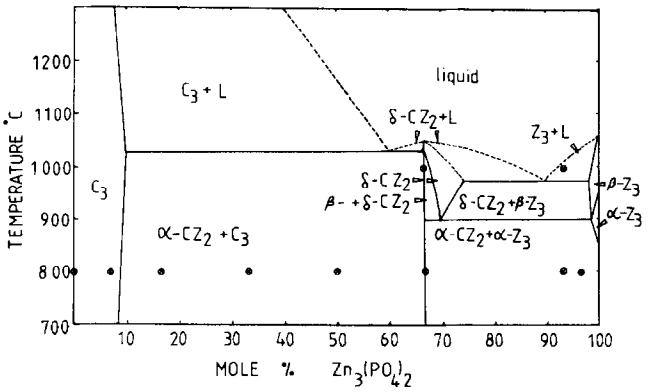

FIG. 1. The phase diagram of the system $Ca_{3-x}Zn_x(PO_4)_2$ (after Ref. (*8*)). C_3 = $Ca_3(PO_4)_2$, CZ_2 = $CaZn_2(PO_4)_2$, and Z_3 = $Zn_3(PO_4)_2$.

ment of the nuclei in continuous solids with an investigation of the solid solution $Zn_{3-x}Mg_x(PO_4)_2$ (*7*). In this case the position and intensity of the four resonances, which arise from crystallographically equivalent phosphorus atoms experiencing different local environments, have made possible a quantitative description of the cation distribution over a range of compositions.

An X-ray powder diffraction investigation of the phase diagram of $Ca_{3-x}Zn_x(PO_4)_2$ has shown it to be a complex system containing line phases, regions of solid solutions, and biphasic mixtures (*8*). The end member calcium phosphate, β-$Ca_3(PO_4)_2$, possesses a structure which is complicated by having five different cation sites including one which has only partial occupancy (*9*). The structure of α-$Zn_3(PO_4)_2$, however, is quite different, being a three-dimensional array of interconnected zinc–oxygen and phosphorus–oxygen tetrahedra (*10*). As a result of these structural differences, which stem from differences in the sizes of the zinc and calcium cations, solubility is not expected to be large in the end members. The reported solubility of zinc phosphate in β-$Ca_3(PO_4)_2$ is 10 mole% while that of calcium phosphate in α-$Zn_3(PO_4)_2$ is less than 1%. At intermediate compositions, a compound of stoichiometry $CaZn_2(PO_4)_2$ is formed in which there is no apparent solubility of either end members. Hence in a large proportion of the phase diagram there is a mixture of two phases, one being the end member solid solution and the other being α-$CaZn_2(PO_4)_2$. A modified version of the phase diagram of the $Ca_{3-x}Zn_x(PO_4)_2$ system, deduced from X-ray powder work by Kreidler and Hummel (*8*), is shown in Fig. 1. This illustrates these features and emphasizes the extent of the biphasic regions.

In this study we present a detailed investigation of the $Ca_{3-x}Zn_x(PO_4)_2$ system by ^{31}P MASNMR. The system was chosen because of its complexity, exhibiting a region of solid solution, two biphasic regions, and an intermediate line phase. It offers an excellent opportunity for assessing the relative merits of MASNMR and classical powder diffraction methods in the elaboration of a complex phase diagram.

Experimental

Powder samples of members of the phase diagram $Ca_{3-x}Zn_x(PO_4)_2$ were prepared by mixing stoichiometric quantities of the salts $CaCO_3$, ZnO, and $NH_4H_2PO_4$ in dilute nitric acid solutions. The solutions were dried

and the resulting powders ground and fired at 800°C for approximately 24 hr. A variety of compositions from x = 0 to 3 were prepared, all of which were white polycrystalline powders. X-ray powder patterns were obtained from all samples to check for impurities. The ^{31}P MASNMR spectra were obtained on a Bruker CXP200 spectrometer operating at 81.0 MHz. Approximately 400-mg samples were used in Delrin Andrews-type rotors. A range of spinning speeds (1.5–4 kHz) was employed with an initial 5-μsec pulse followed by a recycle delay time set according to the required conditions. In general these incorporated a recycle delay time sufficient to obtain full relaxation of the phosphorus atoms in the sample, this being 10 sec for β-$Ca_3(PO_4)_2$ and up to 500 sec for α-$CaZn_2(PO_4)_2$ and $Zn_3(PO_4)_2$ because of the longer spin-lattice relaxation times of phosphorus in the latter compounds. Chemical shifts were measured with respect to an external reference of 85% H_3PO_4 and are reported as taking upfield as negative.

Results and Discussion

(*i*) *An Overview of the $Ca_{3-x}Zn_x(PO_4)_2$ System*

Figure 2 shows the isotropic regions of the ^{31}P MASNMR spectra of preparations with x = 0.0, 0.2, 0.4, 1.0, 1.5, 2.0, 2.6, and 2.9, from the phase diagram $Ca_{3-x}Zn_x(PO_4)_2$. The positions of these samples with respect to the phase diagram are indicated by small circles in Fig. 1. These spectra illustrate the three main regions of the phase diagram, namely, the β-$Ca_3(PO_4)_2$ solid solution, the biphasic mixture of the intermediate composition $CaZn_2(PO_4)_2$ with the β-$Ca_3(PO_4)_2$ solid solution, and the mixture of $CaZn_2(PO_4)_2$ with α-$Zn_3(PO_4)_2$. The samples with x = 0 (pure β-$Ca_3(PO_4)_2$), x = 0.2, and x = 0.4 are dominated by the resonances of the solid solution of $Ca_3(PO_4)_2$ with zinc. However, in the x = 0.4 spectrum there is already a new peak discernable at 10.0 ppm and this grows rapidly as x increases so that by x = 1.0 it is a dominant feature. In fact this peak at 10.0 ppm is clearly accompanied by another resonance at 2.2 ppm. These two peaks (which, when integrated together with the spinning sidebands, give a one-to-one intensity ratio (*6*)) are from the intermediate phase of stoichiometry $CaZn_2(PO_4)_2$. The samples with x = 1.0 and x = 1.5, therefore, illustrate the biphasic region containing the $Ca_3(PO_4)_2$ solid solution and the $CaZn_2(PO_4)_2$ phase. It is noticeable that in these two samples the resonances from $CaZn_2(PO_4)_2$ are significantly broader than in the sample of x = 2.0. This may result from intergrowth of the two phases at a microscopic level, a possibility that is supported by the width of the X-ray powder diffraction lines and by the inhomogeneity (from X-ray microanalysis in an electron microscope) of crystallites smaller than 1 μm in size. The samples of x = 2.6 and x = 2.9 are from the biphasic region between $CaZn_2(PO_4)_2$ and $Zn_3(PO_4)_2$; pure α-$Zn_3(PO_4)_2$ gives a single ^{31}P MSNMR resonance at 3.9 ppm (*7*) and this peak is seen to grow to dominate the spectrum of the sample with x = 2.9. The spectra of the various component phases will now be studied in greater detail.

(*ii*) *The Region of Solid Solution in β-$Ca_3(PO_4)_2$*

The ^{31}P MASNMR spectra of the pure sample of β-$Ca_3(PO_4)_2$ (Fig. 2, x = 0) indicates that it is made up from at least three isotropic resonances of different chemical shift and intensities. This reflects the complex nature of the β-$Ca_3(PO_4)_2$ structure in which there are three crystallographically distinct phosphorus positions (*9*), but in order to interpret the spectrum we must examine the structure in greater detail. The relative occupancies of the three phosphorus positions are 1:3:3 for

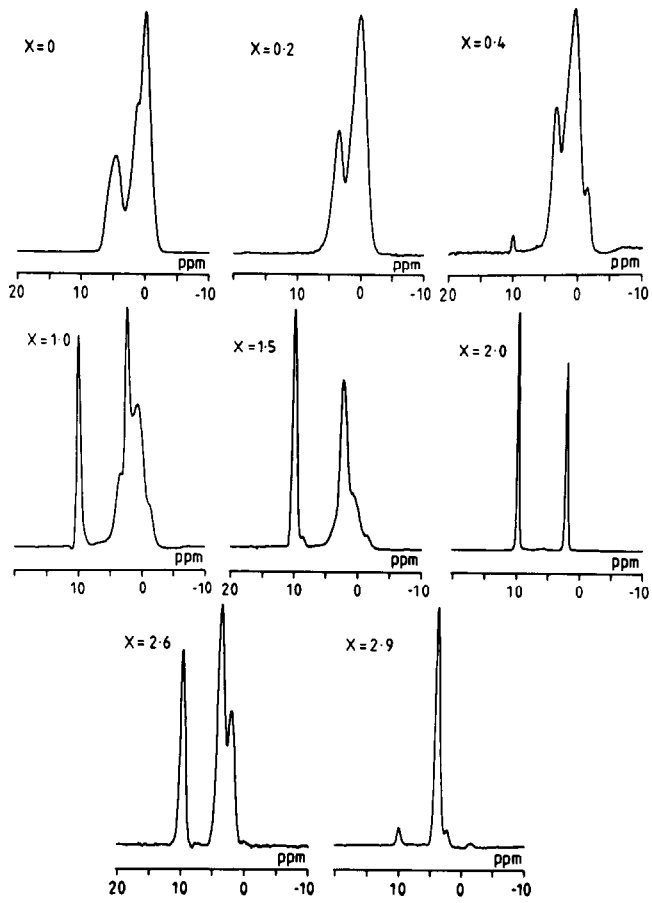

FIG. 2. The isotropic region of the ^{31}P MASNMR spectra of samples from the system $Ca_{3-x}Zn_x(PO_4)_2$ with $x = 0$ (β-$Ca_3(PO_4)_2$), 0.2, 0.4, 1.0, 1.5, 2.0, 2.6, ad 2.9. Spinning speeds of ca. 3 kHz were used to reduce the intensities of the sidebands (not shown) to a few percentage of the total intensity.

P(1) : P(2) : P(3), because P(1) is on a crystallographic special position. The cations are distributed over five different sites and of these, Ca(1), Ca(2), and Ca(3) are general positions having eight or nine coordination and normal Ca–O bond lengths (2.44–2.54 Å). The other two cation sites, Ca(4) and Ca(5), are quite different and are both special positions giving them an effective occupancy of 1/3 of the other cation sites. Ca(5) is a small site on the threefold axis with approximately octahedral coordination; the Ca–O bond lengths are only 2.238 and 2.287 Å. The Ca(4) site further complicates the structure because it is only half occupied, resulting in the relative occupancies of the five cation sites Ca(1) to Ca(5) being 1 : 1 : 1 : 1/6 : 1/3, respectively. The geometry of Ca(4) is quite distorted and there are nine Ca–O bonds: (all ×3) –O(1) 2.538 Å, –O(9) 3.041 Å, and –O(2) 3.228 Å.

In view of the known sensitivity of ^{31}P isotropic chemical shifts to local structural features, we now ask the question: how will the partial occupancy of the Ca(4) site affect the environments of the phosphorus atoms? The oxygen coordination and the connections to the nearest cations about the three phosphorus atoms in the β-$Ca_3(PO_4)_2$ structure are shown in Fig. 3. It can be seen

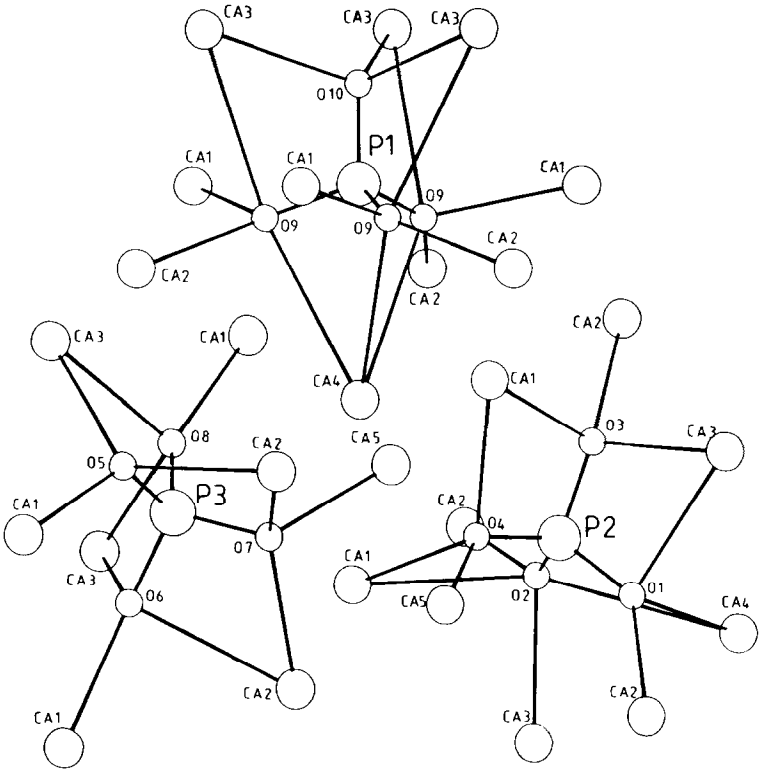

FIG. 3. The coordination around the three phosphorus atoms in β-$Ca_3(PO_4)_2$. All "next-nearest" cations are shown.

that P(3) has no next-nearest Ca(4) cation and therefore, to a first approximation, will not be affected by the occupation of that site. The situations for P(1) and P(2) are quite different. The $P(1)O_4$ tetrahedron shares a common face with a Ca(4) site and its geometry must differ according to whether this is occupied or not. P(2) is also connected to a Ca(4) site, in this case by edge sharing of the $P(2)O_4$ unit. The Ca(4)–O(1) bond length is 2.54 Å, while the Ca(4)–O(2) is much longer, at 3.23 Å. It seems probable then that, as a consequence of the half occupancy of Ca(4), the P(1) and P(2) ^{31}P MASNMR resonances will be split into two equally intense signals (one from a phosphorus next to a vacancy and the other next to a cation on Ca(4)). This will then give five isotropic resonances in all, with relative intensities 1/2 and 1/2 (the P(1) resonances), 3/2 and 3/2 (the P(2) resonances), and 3 (the P(3) resonance). The observed spectrum of β-$Ca_3(PO_4)_2$ is compared in Fig. 4 to a simulated spectrum, calculated using five Gaussian peaks with these relative intensities. The positions of the resonances and their linewidths were adjusted arbitrarily in order to optimize the fit. Of these five resonances the two lowest intensity peaks are not resolvable in the spectra but are necessary to achieve the fit. A schematic diagram of this simulation is shown below.

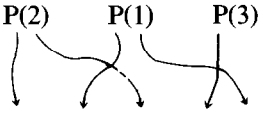

Intensity:	3/2	1/2	3/2	3	1/2
Relative intensity: (%)	21.5	7	21.5	43	7

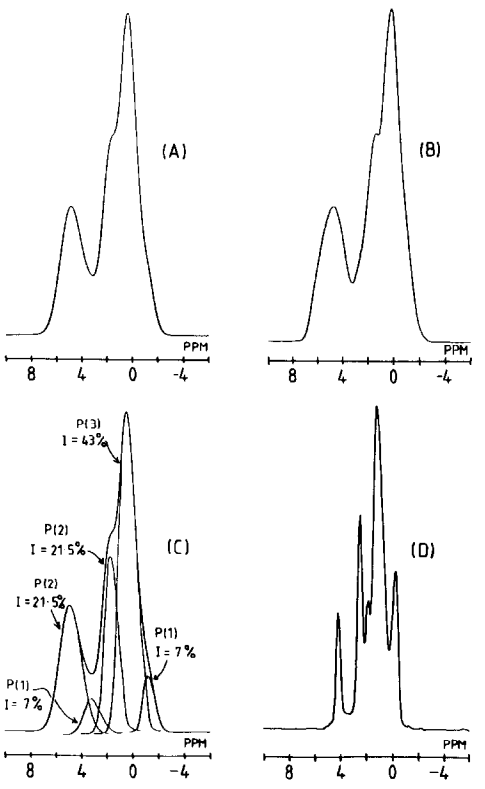

FIG. 4. ^{31}P MASNMR spectra of β-$Ca_3(PO_4)_2$: (A) observed, (B) simulated, and (C) relative intensities of the five component Gaussians used in the simulation, with the allocation to phosphorus atoms in the structure (see text). (D) The ^{31}P MASNMR spectrum of α-$Ca_3(PO_4)_2$.

The resonances obtained from the simulation are much broader than those found with other zinc and calcium phosphates and, indeed, some lines are broader than others. This can probably be attributed to positional disorder of the phosphorus atoms arising from the partial occupancy of the Ca(4) site, a view that is corroborated by the observation of significantly narrower lines for α-$Ca_3(PO_4)_2$ (Fig. 4), in which no such disorder occurs (*11*). The intensities of the spinning sidebands of the individual resonances can provide anisotropic chemical shift data and hence give information about site symmetries. In this study, however, chemical shift anisotropies cannot be obtained because of the extent of overlap of signals in the spinning sidebands.

Substitution of zinc into the β-$Ca_3(PO_4)_2$ structure can only be expected to complicate the picture further, although it might be hoped that the ^{31}P MASNMR spectra may give clues as to where substitution takes place. The ^{31}P MASNMR spectra of $Ca_{3-x}Zn_x(PO_4)_2$ samples with $x = 0$, 0.2, 0.3 (an additional preparation), and 0.4 are shown together in Fig. 5. This shows the maximum solubility of zinc in β-$Ca_3(PO_4)_2$, as indicated by the emergence of the 10-ppm resonance from a phosphorus of the $CaZn_2(PO_4)_2$ phase, to be reached at about $x = 0.3$ (i.e., 10%). This is in good agreement with the solubilities of 9 and 11% observed by Kreidler and Hummel (*8*) and by Nord (*12*), respectively. As zinc is substituted into the β-$Ca_3(PO_4)_2$ structure, the general

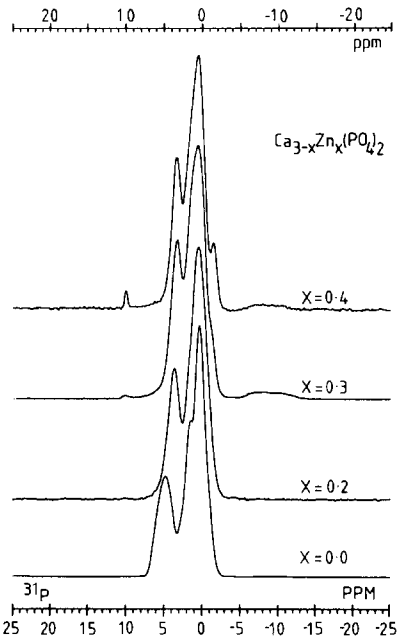

FIG. 5. ^{31}P MASNMR spectra of four samples from the system $Ca_{3-x}Zn_x(PO_4)_2$ with $x = 0$ (β-$Ca_3(PO_4)_2$), 0.2, 0.3, and 0.4; all prepared at 800°C. The broad and weak signal centered at −8 ppm is due to a small amount of $Ca_2P_2O_7$.

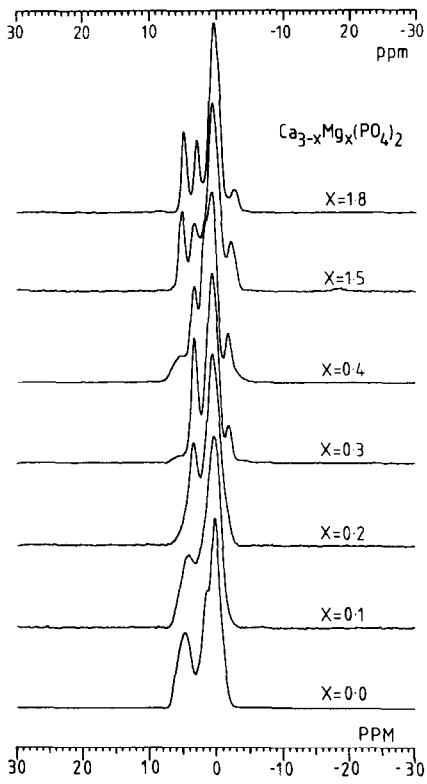

FIG. 6. ^{31}P MASNMR spectra of samples from the system $Ca_{3-x}Mg_x(PO_4)_2$, all prepared at 1000°C.

features of the spectrum change. The downfield ^{31}P resonance narrows and moves upfield (from 5 to 3.5 ppm), a new peak (at about −1.5 ppm) emerges, and the two major peaks of the β-$Ca_3(PO_4)_2$ spectrum appear to move slightly closer together. A detailed explanation of these features, at this stage, would require more structural information concerning the position of cation substitution, but some observations can be made in the light of the tentative allocation of resonances made for the spectrum of β-$Ca_3(PO_4)_2$. The shifting of the peaks in the four spectra shown in Fig. 5 suggests that the P(1) and P(2) resonances are more greatly affected by the zinc substitution than the P(3) resonance. This differential effect points to the zinc substitution being at Ca(4) and/or Ca(5) sites because neither are next-nearest neighbors to P(3), while conversely Ca(1), Ca(2), and Ca(3) sites are next-nearest neighbors to all the phosphorus atoms (see Fig. 3).

There is no crystallographic information available about the cation substitution of zinc into the β-$Ca_3(PO_4)_2$ lattice, but the magnesium system, $Ca_{3-x}Mg_x(PO_4)_2$, which is likely to parallel that of $Ca_{3-x}Zn_x(PO_4)_2$, has been investigated by Schroeder *et al.* (*13*). They concluded that, at low concentrations of magnesium, the cations are statistically distributed over the two cation sites Ca(4) and Ca(5), but that at higher concentrations the cations substitute preferentially at the Ca(5) site. Hence, a crystal with a magnesium substitution of 9.5% ($x = 0.29$) corresponds to one where the Ca(5) sites are filled, because 6 of the 63 sites in the unit cell (9.5%) are Ca(5) sites. The Ca(5) site has near octahedral coordination and might therefore be expected to be the favored site for substitution. Nord (*12*) has suggested that the solubility limit observed in the zinc case is also due to the filling of the Ca(5) site, although in the same study a maximum solubility of only 5% was observed for magnesium substitution in samples prepared at 800°C.

^{31}P MASNMR spectra of samples (with values of $x = 0.0, 0.1, 0.2, 0.3, 0.4, 1.5$, and 1.8) from the phase diagram $Ca_{3-x}Mg_x(PO_4)_2$ are shown in Fig. 6. All samples were prepared by the method described above using stoichiometric quantities of the salts $CaCO_3$, $Mg(NO_3)_2 \cdot 9H_2O$, and $NH_4H_2PO_4$; all samples were fired at 1000°C for 12 hr after drying. The phase diagram given by Ando (*14*) from powder X-ray diffraction gives an approximate maximum solubility of 10% for magnesium substitution. The X-ray powder diffraction patterns of our samples indicate that a pure solid solution exists through to $x = 0.3$ and that the sample with $x = 0.4$ contains a small amount of the phase which dominates

in the samples with $x = 1.5$ and $x = 1.8$. This intermediate phase has a variable stoichiometry resulting from disordered occupancy of some cation sites. The structure has been described as "$Ca_7Mg_9(Ca,Mg)_2(PO_4)_{12}$" (*15*), which therefore has stoichiometry limits of $Ca_{1.5}Mg_{1.5}(PO_4)_2$ and $Ca_{1.2}Mg_{1.8}(PO_4)_2$. Interestingly, this phase is structurally related to α-$Ca_3(PO_4)_2$, the ^{31}P MASNMR spectrum of which is seen in Fig. 4D.

These preparations confirm the maximum solubility of magnesium, at 1000°C, to be in the region of $x = 0.3$. It is striking how similar a progression in features the ^{31}P MASNMR spectra of the magnesium samples ($x = 0.1$ to 0.3, Fig. 6) show to those of the zinc system. That is, the downfield peak narrows and moves upfield, the larger peaks merge, and a new peak at about -2 ppm appears. Again, as in the zinc case, the spectra of the $Ca_{3-x}Mg_x(PO_4)_2$ system indicate that some phosphorus atoms are affected more by the magnesium substitution than others; hence the Ca(4) and Ca(5) sites are once more implicated.

We now consider whether the new resonances in the $Ca_{3-x}Mg_x(PO_4)_2$ ^{31}P MSNMR spectra can be rationalized in terms of the structural details obtained by Schroeder *et al.* (*13*). Examining the local environments of each phosphorus atom in more detail, we can quickly see that many different environments can result for each phosphorus atom when magnesium substitution occurs both at Ca(4) and Ca(5). From the local environments of the phosphorus atoms seen in Fig. 3, it is clear that P(1) will have three possible configurations; one-half of these will be next to a vacancy at Ca(4) and the rest will be next to either a magnesium or a calcium on that site. P(3), on the other hand, is next to one Ca(5) site and so will have two possible configurations, one with magnesium and the other with calcium on Ca(5). P(2), however, is considerably more complicated, having both a neighboring Ca(4) and an Ca(5) site; six configurations are therefore possible. Clearly the superposition of the 11 signals from these different phosphorus atoms is likely to create a complicated spectrum and this may help to account for the broadness of the spectrum with $x = 0.1$ where the cation substitution is thought to be essentially random over the Ca(4) and Ca(5) sites (*13*). However, as the value of x increases from 0.1 to 0.3 the ^{31}P resonances narrow considerably (in fact they do so even with respect to the spectrum of β-$Ca_3(PO_4)_2$). At the value of $x = 0.3$ the cation distribution, according to Schroeder's single-crystal work, has shifted so that the magnesium is now only on the Ca(5) site, and so the Ca(4) site is back to the position of being half-occupied by calcium. This leads to a reduction in the number of local phosphorus environments from 11 to 5. The relative probabilities of these 5 environments are then the same as for the corresponding phosphorus environments in β-$Ca_3(PO_4)_2$, with the Ca(5) site now filled with magnesium instead of calcium.

An analysis of the $x = 0.3$ spectrum (Fig. 6) shows that the downfield peak has an intensity of approximately 28% and the small upfield peak of approximately 7%. A simulation of this spectrum using three Gaussian peaks of relative intensity 28.5 : 64.5 : 7 (i.e., 21.5 + 7 : 21.5 + 43 : 7) is compared to the observed spectrum in Fig. 7, confirming these intensities as being accurate. The simplest explanation of this spectrum is that small shifts in the (isotropic chemical shift) resonances of the five different phosphorus atoms in the initial β-$Ca_3(PO_4)_2$ structure have occurred such that only three peaks can now be resolved.

Returning now to the zinc-containing solid solution, it seems certain that the strong similarity between the ^{31}P MASNMR spectra of the magnesium and the zinc phases arises because of a similar pattern of cation substitution. That is to say

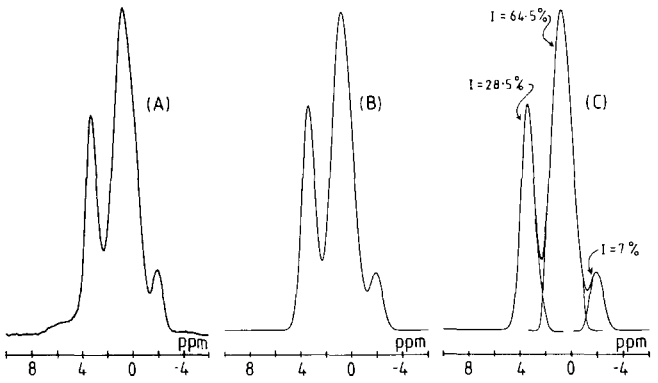

FIG. 7. ^{31}P MASNMR spectra of a sample of stoichiometry $Ca_{2.7}Mg_{0.3}(PO_4)_2$: (A) observed, (B) simulated, and (C) relative intensities of the component Gaussians in this simulation.

that the solubility limit ($x = 0.3$) is reached when zinc occupies all Ca(5) sites.

In the magnesium system, Schroeder *et al.* (*13*) found, at the high temperatures used for his crystal growth, solid solution to about 14% of cation substitution, well beyond the limit of 9% reached when Ca(5) is filled. Although there is no crystallographic information regarding the position of further substitution, it is reasonable to assume that most of this additional magnesium will be found on the Ca(4) site (the Ca(4) and Ca(5) sites together are 6 + 3 of the 63 sites in the unit cell, giving a limit of $x = 0.43$, 14%). In order to test this hypothesis, three samples of the zinc system, with $x = 0.3$, 0.4, and 0.5, were refired at 1300°C and the ^{31}P MASNMR spectra from these samples are shown in Fig. 8. The first thing that is apparent is that the resonance at 10.0 ppm (due to the intermediate phase, $CaZn_2(PO_4)_2$) is no longer present in the spectrum of the $x = 0.3$ sample, although it is still in evidence in the $x = 0.4$ sample. This confirms that there is solubility beyond the Ca(5) site limit. Furthermore, both the lack of change in the general form of the resonances as x increases from 0.3 and the appearance of a limit at approximately $x = 0.4$ is consistent with substitution at the Ca(4) site. Substitution at Ca(1), Ca(2), or Ca(3) would be expected to lead to a higher solubility limit and to cause a more general broadening of the spectrum.

(*iii*) *The Intermediate Composition* $CaZn_2(PO_4)_2$

At a stoichiometry of $x = 2.0$ there exists an apparently pure phase, which gives

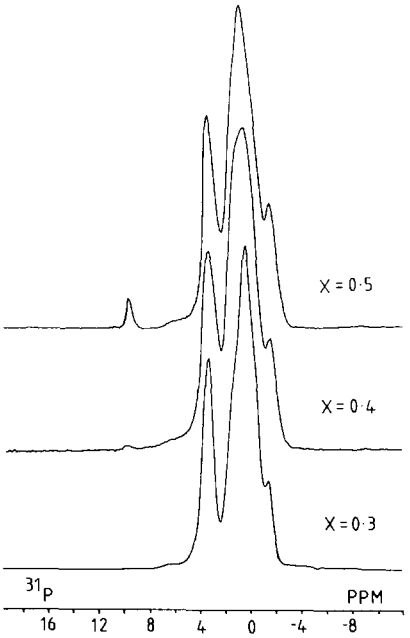

FIG. 8. ^{31}P MASNMR spectra of three samples from the system $Ca_{3-x}Zn_x(PO_4)_2$ with $x = 0.3$, 0.4, and 0.5 (all prepared at 1300°C).

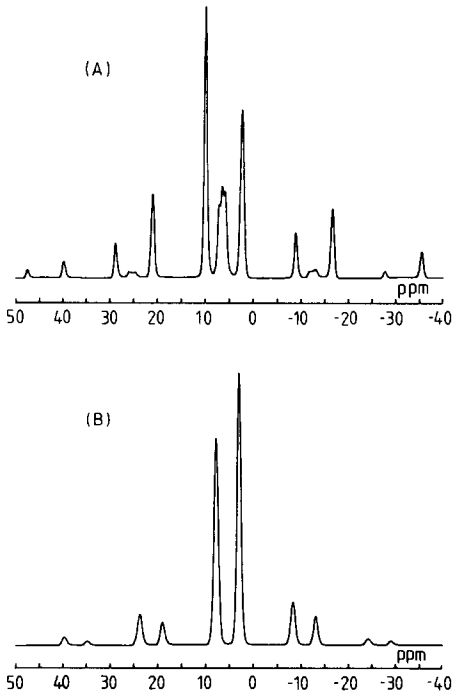

FIG. 9. Slow spinning ^{31}P MASNMR spectra of (A) a mixture of α- and δ-$CaZn_2(PO_4)_2$ at 1520 Hz, and (B) β-$Zn_3(PO_4)_2$ at 1290 Hz.

(when the spinning sidebands are included) two peaks of equal intensity in its ^{31}P MASNMR spectra. There is no observable region, on either side of this composition, where only these two peaks (at 2.2 and 10.0 ppm) are found, and therefore no significant solid solution with zinc or calcium phosphates can exist. This has been confirmed by X-ray powder diffraction (*8*), and the intermediate phase, which exists below 1000°C, has been named the α-form. Above approximately 1000°C, there is another form, δ-$CaZn_2(PO_4)_2$, which can be quenched to room temperature. The ^{31}P MASNMR spectrum of a sample of $CaZn_2(PO_4)_2$, prepared at 1050°C and cooled rapidly to room temperature, shows a mixture of the two phases (Fig. 9). The δ-phase appears to give three isotropic resonances close to 6 ppm, but no further structural details are available. An X-ray single-crystal structure determination and a complementary ^{31}P MASNMR analysis of α-$CaZn_2(PO_4)_2$ is the subject of a separate discussion (*16*).

(*iv*) *The Zinc Phosphate Rich Region of the Phase Diagram*

This is the region of the phase diagram with $2 < x < 3$. An inspection of the spectrum of a sample of stoichiometry $Ca_{0.1}Zn_{2.9}(PO_4)_2$ (see Fig. 2) indicates that the solubility of calcium phosphate in the α-$Zn_3(PO_4)_2$ structure must be very small. For a sample with stoichiometry $Ca_{0.5}Zn_{2.5}(PO_4)_2$ the spectrum gives three isotropic resonances, one at 10.0 ppm and two overlapping at 3.9 and 2.2 ppm. A comparison of the integrated intensities of these two groups shows that, to within experimental error, the ratio of intensities is 1 : 3.0. There is, therefore, no observable solution of $Ca_3(PO_4)_2$ in α-$Zn_3(PO_4)_2$, a result in agreement with Kreidler's study (*8*).

Above 942°C α-$Zn_3(PO_4)_2$ is converted to a second phase, β-$Zn_3(PO_4)_2$, which is metastable at room temperature. β-$Zn_3(PO_4)_2$ has two phosphorus atoms in the asymmetric unit (*17*), as is confirmed by the two peaks in the ^{31}P MASNMR spectrum in Fig. 9B. The β-$Zn_3(PO_4)_2$ structure will dissolve more calcium phosphate than the α-phase and this is illustrated by the ^{31}P MASNMR spectrum of the stoichiometry $Ca_{0.07}Zn_{2.93}(PO_4)_2$, prepared by firing at 1000°C and cooling rapidly to room temperature. This spectrum, seen in Fig. 10A, shows only two resonances due to the β-$Zn_3(PO_4)_2$ solid solution; the solubility (approximately 2%) is close to that observed by Kreidler (1.5%). In the composition $Ca_{0.2}Zn_{2.8}(PO_4)_2$ (Fig. 10B) the limit of solution has been exceeded, as indicated by the emergence of resonances from δ-$Ca Zn_2(PO_4)_2$ at around 6 ppm in the ^{31}P MASNMR spectrum.

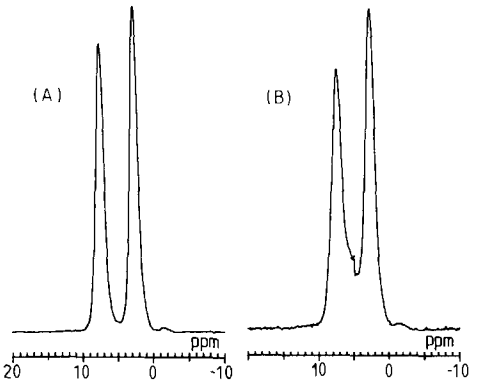

FIG. 10. ^{31}P MASNMR spectra of (A) the stoichiometry $Ca_{0.07}Zn_{2.93}(PO_4)_2$ and (B) the stoichiometry $Ca_{0.2}Zn_{2.8}(PO_4)_2$. Both samples were prepared at 1000°C.

Conclusion

This study of the $Ca_{3-x}Zn_x(PO_4)_2$ system by ^{31}P MASNMR has demonstrated how this technique may be used to investigate a complex system which contains solid solutions, line phases, and regions of biphasic mixtures. We have found that solubility of $Zn_3(PO_4)_2$ in the β-$Ca_3(PO_4)_2$ phase is in excellent agreement with previous work by powder diffraction methods and that the sensitivity of the two approaches is very similar. In the present instance, the MASNMR study provides additional detail relating to the mode of substitution of zinc for calcium. By analogy with the $Ca_{3-x}Mg_x(PO_4)_2$ system, for which single-crystal structure information is available, the spectra can be interpreted in terms of preferential substitution at the Ca(5) site. Furthermore, the phase limit is reached when this site has been fully substituted. It is also clear from the MASNMR spectra results that the intermediate phase, α-$CaZn_2(PO_4)_2$, has no range of homogeneity. Given the complexity of the X-ray powder patterns in this system, it is difficult to draw these conclusions with any confidence from classical diffraction data. Similarly, we have confirmed that there is no detectable solution of calcium in α-$Zn_3(PO_4)_2$. X-ray powder methods offer the advantage of providing information about the type of structure adopted by each phase and it should normally be feasible to determine the lattice parameters and crystal system. By contrast, MSNMR provides local information concerning the environment of the NMR active elements. In favorable cases, it may reveal the number of atoms of a particular type in the asymmetric unit and thus help to resolve space group ambiguities. Furthermore, cation distributions may be revealed, as in the system $Zn_{3-x}Mg_x(PO_4)_2$ (7) and, to some extent, in the present work. The most efficacious approach, however, is to use a combination of both methods, taking advantage of their relative strengths and complementarity.

Acknowledgments

The authors thank the SERC for a grant toward purchase of NMR equipment. R.J.B.J. is grateful to B.P. for an EMRA grant and N.J.C. to Shell, Thorton Research Centre for financial assistance.

References

1. J. KLINOWSKI, J. M. THOMAS, C. A. FYFE, AND G. C. GOBBI, *Nature (London)* **286,** 553 (1982).
2. E. LIPPMAA, A. SAMOSON, AND M. MAGI, *J. Amer. Chem. Soc.* **108,** 1730 (1986).
3. C. A. FYFE, G. C. GOBBI, J. KLINOWSKI, J. M. THOMAS, AND S. RAMDAS, *Nature (London)* **296,** 530 (1982).
4. E. LIPPMAA, M. MAGI, A. SAMOSON, G. ENGELHARDT, AND A.-R. GRIMMER, *J. Amer. Chem. Soc.* **102,** 4889 (1980).
5. K. A. SMITH, R. J. KIRKPATRICK, E. OLDFIELD, AND D. M. HENDERSON, *Amer. Mineral.* **68,** 1206 (1983).
6. A. K. CHEETHAM, N. J. CLAYDEN, C. M. DOBSON, AND R. J. B. JAKEMAN, *J. Chem. Soc. Chem. Commun.*, 195 (1986).
7. R. J. B. JAKEMAN, A. K. CHEETHAM, N. J. CLAYDEN, AND C. M. DOBSON, *J. Amer. Chem. Soc.* **107,** 6249 (1985).

8. E. R. KREIDLER AND F. A. HUMMEL, *Inorg. Chem.* **6,** 524 (1967).
9. B. DICKENS, L. W. SCHROEDER, AND W. E. BROWN, *J. Solid State Chem.* **10,** 232 (1974).
10. C. CALVO, *Canad. J. Chem.* **43,** 436 (1965).
11. M. MATHEW, L. W. SCHROEDER, B. DICKENS, AND W. E. BROWN, *Acta Crystallogr. Sect. B* **33,** 1325 (1977).
12. A. G. NORD, *Neues Jahrb. Mineral.*, 489 (1983).
13. L. W. SCHROEDER, B. DICKENS, AND W. E. BROWN, *J. Solid State Chem.* **22,** 253 (1977).
14. J. ANDO, *Bull. Chem. Soc. Japan* **31,** 196 (1957).
15. B. DICKENS AND W. E. BROWN, *Mineral. Petrogr. Mitt.* **16,** 79 (1971).
16. R. J. B. JAKEMAN AND A. K. CHEETHAM, *J. Amer. Chem. Soc.* **110,** 1140 (1988).
17. J. S. STEPHENS AND C. CALVO, *Canad. J. Chem.* **45,** 2303 (1967).